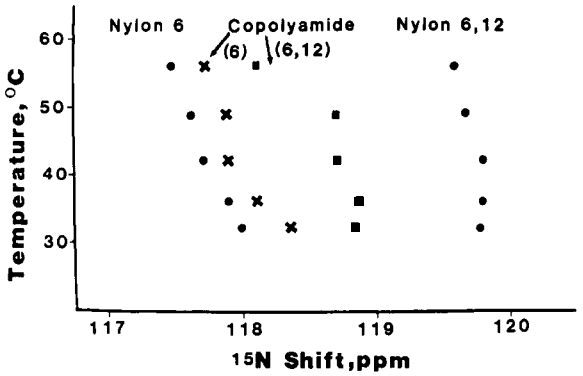

Figure 3. ^{15}N chemical shifts of polyamides in trifluoroacetic acid vs. temperature. The nylon 6,12 component of the copolymer shifts upfield at higher temperatures.

temperature dependence of a copolyamide and its two components, 6 and 6,12. Figure 3 is a plot of temperature vs. ^{15}N chemical shifts of nylons 6 and 6,12 and of the copolyamide (85% 6,12/15% 6) in TFA. Nylons 6 and 6,12 as well as the 6 component of the copolymer showed little temperature dependence from 31 to 56 °C. The 6,12 component showed little dependence up to 49 °C and then shifted upfield at 56 °C, approaching the 6 component. The chemical shift differences ($\Delta\delta$) for nylon 6 and the 6 component were 0.6–0.7 ppm while $\Delta\delta$ for nylon 6,12 was 0.2 ppm from 31 to 56 °C (Table II). For the 6,12 component of the copolymer, $\Delta\delta$ was 0.2 ppm over the 31–49 °C temperature range; from 49 to 56 °C, however, $\Delta\delta$ for the 6,12 component was 0.6 ppm. The large shift seems to indicate a conformational change as opposed to a degradation since data collected following the high-temperature measurements were in very good agreement with data collected prior to elevation of temperature to 56 °C. The change apparently decreases the extent of protonation and/or decreases the basicity of the amide groups since the amide signal of the 6,12 component shifts upfield toward the signal of the shorter chain, less basic 6 component of the copolyamide. Since there was no appreciable change in the ratio of peak intensities for the copolyamide, there should not have been an appreciable increase in the rate of proton exchange at the NH of the amide. Further temperature studies may reveal whether TFA acts as the Θ solvent for the copolyamide at elevated temperatures.

Conclusions

Utilizing the J cross-polarization technique in liquids has allowed us to undertake experiments formerly impractical for ^{15}N NMR: a decrease in experimental time by a factor of 100 was demonstrated. We have differentiated the ^{15}N chemical shifts of a copolyamide and extended the measurements of ^{15}N chemical shifts in nylon *n* and nylon 6,*n* polyamides. We have determined solvent and concentration dependences of nylon ^{15}N chemical shifts and studied the effect of temperature on a copolyamide and its component nylons.

Our data imply that, in the presence of excess acid, protonation and/or hydrogen bonding takes place at the oxygen of the amide carbonyl. As a result, the nitrogen is deshielded and the ^{15}N signal shifts downfield with increasing acid strength. As the amide/acid ratio approaches 1/1 in strong acids, however, our results show an increase in the rate of proton exchange at the NH of the amide and an upfield shift of ^{15}N signal in the nylon 66/TFA solution.

The amount of information which can be gained relating to nitrogen chemistry would be a boon not only for nylons and other industrial products but in the field of biochemistry as well, where nitrogen is a most common element and samples are often small. In the case of fast proton exchange, the system could be cooled and observed in the region of slow exchange as necessary.

References and Notes

(1) Kricheldorf, H. R.; Hull, W. E. *J. Polym. Sci., Polym. Chem. Ed.* **1978**, *16*, 583.
(2) Bertrand, R. D.; Moniz, W. B.; Garroway, A. N.; Chingas, G. C. *J. Am. Chem. Soc.* **1978**, *100*, 5227. *J. Magn. Reson.* **1978**, *32*, 465.
(3) Gordon, A. J.; Ford, R. A. "The Chemist's Companion"; Wiley: New York, 1972. Hexafluoroisopropyl alcohol data from E. I. du Pont and Co. data sheets.
(4) Kricheldorf, H. R.; Schilling, G. *Makromol. Chem.* **1978**, *179*, 2667.
(5) Kricheldorf, H. R. *Makromol. Chem.* **1978**, *179*, 2675.
(6) Kricheldorf, H. R., private communication (to R. C. Ferguson).
(7) Kricheldorf, H. R. *Makromol. Chem.* **1978**, *179*, 2687.
(8) Schilling, G.; Kricheldorf, H. R. *Makromol. Chem.* **1975**, *176*, 3341.
(9) Stewart, W. E.; Mandelkern, L.; Glick, R. E. *Biochemistry* **1967**, *6*, 150. Bovey, F. A. "High Resolution NMR of Macromolecules"; Academic Press: New York, 1972; pp 282–6.

Determination of Short-Chain Branching in Polyethylenes by Pyrolysis–Hydrogenation Glass Capillary Gas Chromatography

Yoshihiro Sugimura, Takao Usami, Tamio Nagaya, and Shin Tsuge*

Department of Synthetic Chemistry, Faculty of Engineering, Nagoya University, Nagoya 464, Japan. *Received February 4, 1981*

ABSTRACT: Pyrolysis–hydrogenation glass capillary gas chromatography was applied to the determination of the short branches in low-density polyethylenes (LDPE). The relative peak intensities of characteristic key isoalkanes in the C_{11} region such as 4-methyl-C_{10} for methyl branches, 3-methyl-C_{10} for ethyl branches, and 5-methyl-C_{10} for butyl branches were correlated with the associated short branch contents in LDPE's by comparing the data of reference model ethylene–α-olefin copolymers with known short branch contents. As a whole, butyl branches are most abundant, ethyl branches occur less frequently, and methyl branches are only a minor structural feature along the polymer chain of LDPE's. The estimated total branch contents for various LDPE's were in fairly good agreement with those obtained by the conventional IR method. The possibility of estimating amyl branch contents was also discussed.

Since the first report on the branches along the polymer chain in polyethylene (PE) by Fox and Martin[1] in 1940, various analytical methods have been adopted for characterization of chain branching. Among these are IR,[2-5] ^1H NMR,[6] ^{13}C NMR,[7-10] γ radiolysis,[2,11,12] and pyrolysis–hydrogenation gas chromatography (PHGC).[13-22]

Earlier work with a packed separation column[13,14] showed that PHGC was a very promising technique for

0024-9297/81/2214-1787$01.25/0

Table I
Possible Fragmentation Products from the Site of Branching in PE

carbon no.	short branches in PE	fragmentation products formed through scissions at ω and α, ..., ω and μ [a]												total kinds of isoalkanes
		α	β	γ	δ	ε	ζ	η	θ	ι	κ	λ	μ	
C_8	methyl	N	2M	3M	4M	3M	2M	N						4
	ethyl	N	3M	3E	3E	3M	N							
	butyl	N	3M	3M	N									
	amyl	N	2M	N										
C_9	methyl	N	2M	3M	4M	4M	3M	2M	N					5
	ethyl	N	3M	3E	4E	3E	3M	N						
	butyl	N	4M	3E	4M	N								
	amyl	N	3M	3M	N									
C_{10}	methyl	N	2M	3M	4M	5M	4M	3M	2M	N				6
	ethyl	N	3M	3E	4E	4E	3E	3M	N					
	butyl	N	5M	4E	4E	5M	N							
	amyl	N	4M	3E	4M	N								
C_{11}	methyl	N	2M	3M	4M	5M	5M	4M	3M	2M	N			8
	ethyl	N	3M	3E	4E	5E	4E	3E	3M	N				
	butyl	N	5M	5E	4P	5E	5M	N						
	amyl	N	5M	4E	4E	5M	N							
C_{12}	methyl	N	2M	3M	4M	5M	6M	5M	4M	3M	2M	N		10
	ethyl	N	3M	3E	4E	5E	5E	4E	3E	3M	N			
	butyl	N	5M	5E	5P	5P	5E	5M	N					
	amyl	N	6M	5E	4P	5E	6M	N						
C_{13}	methyl	N	2M	3M	4M	5M	6M	6M	5M	4M	3M	2M	N	11
	ethyl	N	3M	3E	4E	5E	6E	5E	4E	3E	3M	N		
	butyl	N	5M	5E	5P	5B	5P	5E	5M	N				
	amyl	N	6M	6E	5P	5P	6E	6M	N					

[a] N = *n*-alkanes, 2M = 2-methylalkanes, 3E = 3-ethylalkanes, 4P = 4-propylalkanes, and 5B = 5-butylalkanes.

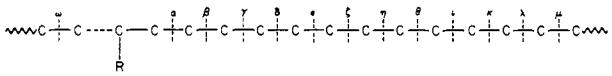

R = short branches

studying the branch structure of polyolefins. Later, a firm relationship between chain branching in the polymer backbone and the degradation products appearing on pyrograms of PE was established by Seeger et al.[15-17] In more recent work using a capillary separation column,[18-22] the resolution of pyrograms has been drastically improved. Thus, PHGC is now approaching the stage where a fairly detailed interpretation of the short branches in PE can be made from high-resolution pyrograms. Moreover, PHGC, among the methods mentioned, has a higher sensitivity than the other methods for detecting short branches even at concentrations as low as a few per 10 000 CH_2 units.[20]

In our recent work,[21,22] the high-resolution pyrograms of PE's by PHGC were interpreted in terms of qualitative and semiquantitative analysis of short branching. In this paper, a method for quantitative estimation of short branching in PE is proposed by simulating the isoalkane fragmentation pattern of PE using patterns of reference model polymers with known short branching. Thus, the estimated values for seven commercially available low-density PE's (LDPE) were in fairly good agreement with those measured by the conventional IR method.[3]

Experimental Section

Materials. Two types of commercial PE's were used: (a) seven LDPE's with densities of 0.935, 0.931, 0.928, 0.924, 0.921, 0.920, and 0.919 and (b) a high-density (0.963) PE (HDPE). Three types of ethylene–α-olefin copolymers from various commercial sources were used: (a) two ethylene–propylene copolymers (P(E-co-P)) with 4.01 and 0.91 mol % propylene, (b) two ethylene–1-butene copolymers (P(E-co-B)) with 3.62 and 0.76 mol % 1-butene, and (c) two ethylene–1-hexene copolymers (P(E-co-H)) with 3.50 and 1.40 mol % 1-hexene. Samples of P(E-co-P), P(E-co-B), and P(E-co-H) with a higher content of comonomers were used as model polymers with known short branching: 20.1 methyl groups/1000 CH_2, 18.1 ethyl groups/1000 CH_2, and 17.5 butyl groups/1000 CH_2, respectively.

PHGC Conditions. PHGC conditions were basically the same as those described elsewhere.[21,22] A vertical microfurnace-type pyrolyzer (Yanagimoto, GP-1018) was directly attached to a gas chromatograph (Shimadzu, 7AG) with a glass capillary column (0.9-mm o.d. × 0.3-mm i.d. × 50 m long, OV-101 (SCOT)) and FID. The column temperature was programmed from 40 to 250 °C at a rate of 2 °C/min. A hydrogenation catalyst column maintained at 200 °C was inserted between the pyrolyzer and the splitter with a splitting ratio of 1:70. Samples of 300 μg were pyrolyzed at 650 °C under a flow of carrier gas (50 mL of H_2/min).

IR Conditions. Although it is known that the extinction coefficient for methyl groups will be different depending on the branch length,[4] the total methyl contents in LDPE's were simply estimated from the absorption band at 1378 cm^{-1} after a correction was made for methylene absorptions at 1368, 1352, and 1303 cm^{-1} by the method proposed by Shirayama et al.[3] The contributions of methyl end groups in the polymer chain were neglected.

Results and Discussion

Figure 1 shows typical high-resolution pyrograms of (A) HDPE, (B) LDPE, and the model polymers as (C) P(E-co-P), (D) P(E-co-B), and (E) P(E-co-H) obtained by the pyrolysis–hydrogenation method. The minor peaks between the serial main peaks of *n*-alkanes are mostly isoalkanes which are closely related to the short branching in the polymer chains. Table I summarizes the possible fragmentation products from C_8 to C_{13} in PHGC formed from the following model segment of the branching structures in the polymer chain:

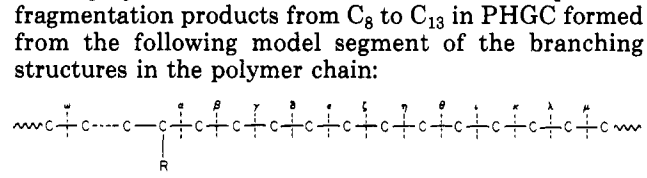

Here, R represents short branches ($CH_3(CH_2)_n$, n = 0, 1,

Table II
Observed Correlation Factors for Model Polymers

model polymer	branch content per 1000 CH_2	key peak intensity[a]	calcd correlation factor
P(E-co-P)	20.1 methyl	$I(4M)_{obsd}$ = 28.2	f_M = 713
P(E-co-B)	18.1 ethyl	$I(3M)_{obsd}$ = 46.8	f_E = 387
P(E-co-H)	17.5 butyl	$I(5M)_{obsd}$ = 35.0	f_B = 500

[a] Values relative to $I(n\text{-}C_{11})_{obsd}$ = 1000.

3, or 4). The listed products in Table I are formed through scission at ω and α, ω and β, ... and ω and μ bonds followed by hydrogenation of the olefinic double bonds in the products, where only scissions along the main chain were taken into consideration. In the following discussion, propyl branches were not taken into consideration since most of the IR and NMR studies showed them to be absent in LDPE.

Theoretically, the higher carbon number regions provide information up to the longer short branches in PE. On the other hand, the number of possible isoalkanes becomes larger in the higher region which, in turn, makes the complete separation of the associated isoalkanes harder even when a high-resolution capillary column is used. Here, the most characteristic peaks for methyl, ethyl, butyl, and amyl branches are formed through ω and β scissions: 2-methyl (above C_4), 3-methyl (above C_6), 5-methyl (above C_{10}), and 6-methyl (above C_{12}) isoalkanes, respectively. However, under our experimental conditions, the peak resolution above C_{12} was insufficient for separation of the isoalkanes. Accordingly, the following discussion is mostly developed for methyl, ethyl, and butyl branches by using the C_{11} region. Thus Figure 2 illustrates the expanded portions of the pyrograms around the C_{11} region.

Fragmentation of Model Polymers. As was expected from Table I, P(E-co-P) yields isoalkanes such as 2M, 3M, 4M, and 5M whose relative intensities are about 2:1:1:1, respectively. Therefore the relative probabilities ($P(\cdots)$) of the cleavages along the backbone can be regarded as $P(\beta) \sim 2P(\gamma) \sim 2P(\delta) \sim 2P(\epsilon)$. In this case, the cleavages at the branches might be negligible. For P(E-co-B), the expected isoalkane peaks of 3M, 3E, 4E, and 5E appear on the pyrogram with relative intensities about 2.3:1:1:1, which means $P(\beta) \sim 2.3P(\gamma) \sim 2.3P(\delta) \sim 2.3P(\epsilon)$. However, the additional peaks corresponding to 2M, 4M, and 5M suggest that cleavages along the side chain also occur to some extent. As for P(E-co-H), the expected isoalkane peaks of 5M, 5E, and 4P appear with relative intensities of about 3:1:1, which means $P(\beta) \sim 3P(\gamma) \sim 3P(\delta)$. However, the appearance of additional 3E, 3M, 2M, 4E, and 4M peaks apparently indicates the occurrence of side-chain cleavages.

Estimation of the Short Branch Contents in Copolymers. The most intense key peaks for methyl, ethyl, and butyl branches are 2M, 3M, and 5M, respectively. However, the peak resolution of 2M and 3E was not enough even in the C_{11} region. Therefore, 4M was used as a key peak for methyl branches instead of 2M. Thus, for example, the correlation factor (f_M) for the content of methyl branches with the observed relative peak intensity of 4M ($I(4M)_{obsd}$) was defined as follows:

$$\frac{I(4M)_{obsd}}{I(n\text{-}C_{11})_{obsd}} \times f_M = \text{methyl branch number}/1000\ CH_2 \quad (1)$$

where $I(4M)_{obsd}$ is the relative value when the observed peak intensity of n-C_{11} alkane (undecane) is regarded as 1000 ($I(n\text{-}C_{11})_{obsd}$ = 1000). The value f_M = 713 is calculated by applying this relation to the observed $I(4M)_{obsd}$ = 28.2 for the model polymer P(E-co-P) with 20.1 methyl groups/1000 CH_2. Similarly, for ethyl and butyl branches, the correlation factors (f_E = 387 and f_B = 500) are calculated from the data of the model polymers and listed in Table II. Once these factors are determined, each branch content of the same type of copolymer can easily be estimated from the observed relative peak intensity of the key peak using eq 1. These estimated values are listed in Table III. These data suggest that the relative intensities of the key peaks are quite effective for the estimation of branch contents in the copolymers where it is only necessary to consider a single type of branch.

Estimation of the Amount of Short Branches in LDPE's. The key peaks of 4M for methyl branches, 3M for ethyl branches, and 5M for butyl branches, however,

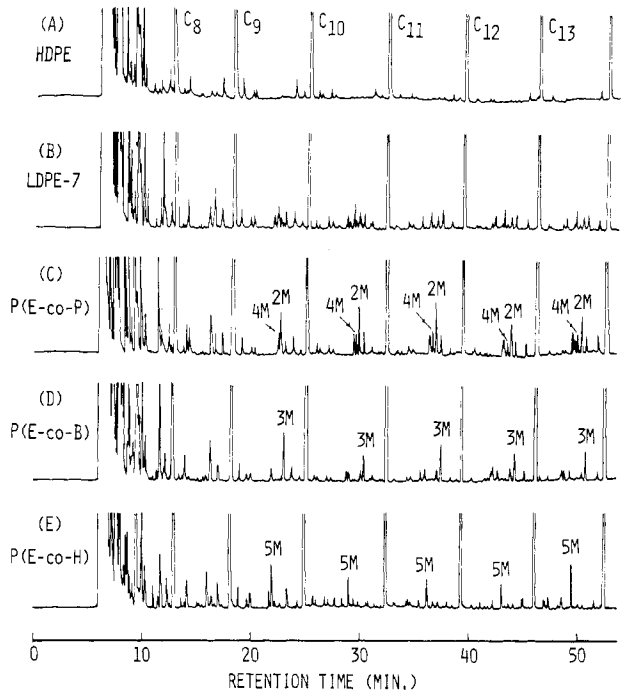

Figure 1. High-resolution pyrograms of HDPE, LDPE, and model copolymers at 650 °C: HDPE, density 0.963; LDPE, LDPE-7 with density 0.919; model copolymers, P(E-co-P) with 4.01 mol % propylene, P(E-co-B) with 3.62 mol % 1-butene, and P(E-co-H) with 3.50 mol % 1-hexene. 2M = 2-methylalkanes, 3M = 3-methylalkanes, 4M = 4-methylalkanes, and 5M = 5-methylalkanes.

Table III
Estimated Branch Contents in Copolymer Samples

sample	branch content per 1000 CH_2 by IR	key peak intensity[a]	correlation factor[b]	estimated branch content per 1000 CH_2
P(E-co-P)	4.7 methyl	$I(4M)_{obsd}$ = 6.5	f_M = 713	4.6 methyl
P(E-co-B)	3.8 ethyl	$I(3M)_{obsd}$ = 9.4	f_E = 387	3.6 ethyl
P(E-co-H)	7.0 butyl	$I(5M)_{obsd}$ = 13.7	f_B = 500	6.8 butyl

[a] Values relative to $I(n\text{-}C_{11})_{obsd}$ = 1000. [b] Calculated in Table II for model polymers.

Table IV
Mutual Participation of Key Peaks from Model Polymers

model polymer	branch content per 1000 CH_2 by IR	relative intensity of key peaks[a]		
		$I(4M)_{obsd}$	$I(3M)_{obsd}$	$I(5M)_{obsd}$
P(E-co-P)	20.1 methyl	28.2 (1.000)	33.0 (1.170)	29.5 (1.045)
P(E-co-B)	18.1 ethyl	4.4 (0.094)	46.8 (1.000)	4.6 (0.098)
P(E-co-H)	17.5 butyl	3.5 (0.100)	6.7 (0.191)	35.0 (1.000)

[a] Values relative to $I(n\text{-}C_{11}) = 1000$. Values in parentheses are values relative to the underlined key peaks.

Table V
Estimated Short Branch Contents in LDPE's

sample	density	total methyl per 1000 CH_2 by IR	relative intensity of key peaks[a]			estimated short branch content per 1000 CH_2			
			$I(4M)_{obsd}$	$I(3M)_{obsd}$	$I(5M)_{obsd}$	methyl	ethyl	butyl	total
LDPE-1	0.935	7.0	2.0	9.4	9.1	0.4	2.8	3.9	7.1
LDPE-2	0.931	10.1	2.5	12.5	12.9	0.3	3.8	5.8	9.9
LDPE-3	0.928	18.9	4.0	14.2	27.0	0.4	3.3	12.8	16.5
LDPE-4	0.924	24.9	4.6	18.3	29.5	0.5	4.7	13.8	19.0
LDPE-5	0.920	26.8	4.8	17.9	31.1	0.6	4.4	14.6	19.6
LDPE-6	0.921	28.5	5.3	23.4	33.6	0.4	6.5	15.7	22.6
LDPE-7	0.919	29.3	9.3	23.1	37.5	3.7	4.3	15.5	23.5

[a] Values relative to $I(n\text{-}C_{11})_{obsd} = 1000$.

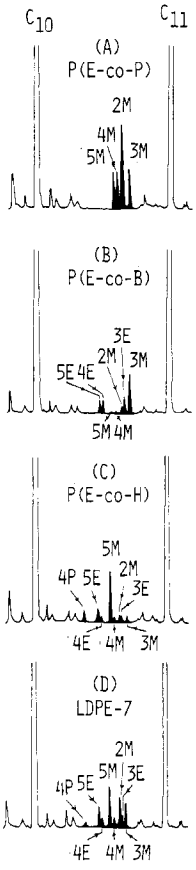

Figure 2. Partial pyrograms of model copolymers and LDPE in the C_{11} region. Model copolymers and LDPE same as in Figure 1. 2M = 2-methyldecane, 3M = 3-methyldecane, 4M = 4-methyldecane, 5M = 5-methyldecane, 3E = 3-ethylnonane, 4E = 4-ethylnonane, 5E = 5-ethylnonane, and 4P = 4-propyloctane.

are not independent of each other. For example, the data in Table I indicate that methyl branches should have some effect on the yield of both 3M and 5M. Moreover, as was discussed above, the side-chain cleavages should also be considered. Therefore, the observed peak intensities (I_{obsd}) of 4M, 3M, and 5M cannot be correlated directly with the associated short branch contents.

Therefore the effective peak intensity, I_{eff}, for each key peak should be calculated by considering the mutual contribution of the other key peaks. Table IV summarizes the relative intensities of the peaks from the model copolymers. Thus the following relations between I_{obsd} and I_{eff} can be adopted:

$$I(4M)_{eff} + 0.094I(3M)_{eff} + 0.100I(5M)_{eff} = I(4M)_{obsd}$$
$$1.170I(4M)_{eff} + I(3M)_{eff} + 0.191I(5M)_{eff} = I(3M)_{obsd} \quad (2)$$
$$1.045I(4M)_{eff} + 0.098I(3M)_{eff} + I(5M)_{eff} = I(5M)_{obsd}$$

Once the effective peak intensities, $I(4M)_{eff}$, $I(3M)_{eff}$, and $I(5M)_{eff}$, are calculated for a given LDPE using the observed peak intensities, $I(4M)_{obsd}$, $I(3M)_{obsd}$, and $I(5M)_{obsd}$, the short branch contents for methyl (C_M), ethyl (C_E), and butyl (C_B) can be obtained by using the correlation factors f_M, f_E, and f_B listed in Table II:

$$C_M = (I(4M)_{eff}/1000) \times f_M$$
$$C_E = (I(3M)_{eff}/1000) \times f_E \quad (3)$$
$$C_B = (I(5M)_{eff}/1000) \times f_B$$

Table V summarizes the observed relative intensities of the key peaks against n-C_{11} alkane and the calculated short branch contents using eq 2 and 3 for the seven kinds of LDPE's. These data suggest that butyl is the most abundant short branch and that ethyl is the second most abundant. This tendency is basically consistent with IR[2-5] and NMR[6-10] results. The content of methyl branches is generally very small, except for LDPE-7. This result suggests, as was pointed out by Axelson et al.,[10] that the LDPE-7 might be synthesized by using propylene as a polymerization modifier. As a whole, the estimated total short branch contents obtained by this method are in fairly good agreement with those obtained by the IR method. However, the observed values for the lower density LDPE's are about 20% less than those obtained by IR measurements. These discrepancies could be attributed mainly to the gross total methyl contents obtained by IR measurements and partly to the neglect of amyl and longer branches by the PHGC method. It is also reported that the branches in LDPE tend to occur in clusters along the polymer chain rather than randomly.[10,12] However, in this work, the theory was developed by assuming that the

branches are randomly situated along the polymer backbone in LDPE. This might have some effect on the observed branch contents obtained by PHGC.

As was discussed in Table I, if we can achieve enough separation of the resulting isoalkanes above the C_{12} region, the amyl branch contents could be determined by PHGC. In that event, the estimated butyl branch contents migh be lower than those in Table V since the data in Table I predict that 5M in the C_{11} region, utilized as the key peak for butyl branches, also is expected to be formed from the amyl branch structure. In addition to the higher resolution of pyrograms, the use of well-studied model polymers is a very important factor in obtaining reliable results. Further work along these lines is currently in progress.

References and Notes

(1) Fox, J. J.; Martin, A. E. *Proc. R. Soc. London, Ser. A* **1940**, *175*, 208.
(2) Willbourn, A. H. *J. Polym. Sci.* **1959**, *34*, 569.
(3) Shirayama, K.; Okada, T.; Kita, S. *J. Polym. Sci., Part A* **1965**, *3*, 907.
(4) Baker, C.; David, P.; Maddams, W. F. *Makromol. Chem.* **1979**, *180*, 975.
(5) Rueda, D. R.; Baltá Calleja, F. J.; Hidalgo, A. *Spectrochim. Acta, Part A* **1979**, *35a*, 847.
(6) Ferguson, R. C. *Macromolecules* **1971**, *4*, 324.
(7) Randall, J. C. *J. Polym. Sci., Polym. Phys. Ed.* **1973**, *11*, 275.
(8) Bovey, F. A.; Schilling, F. C.; McCrackin, F. L.; Wagner, H. L. *Macromolecules* **1976**, *9*, 76. Cheng, H. N.; Schilling, F. C.; Bovey, F. A. *Ibid.* **1976**, *9*, 363.
(9) Culter, D. J.; Hendra, P. J.; Cudby, M. E. A.; Willis, H. A. *Polymer* **1977**, *18*, 1005.
(10) Axelson, D. E.; Levy, G. C.; Mandelkern, L. *Macromolecules* **1979**, *12*, 41.
(11) Kamath, P. M.; Barlow, A. *J. Polym. Sci., Part A* **1967**, *5*, 2023.
(12) Bowmer, T. N.; O'Donnell, J. H. *Polymer* **1977**, *18*, 1032.
(13) Van Schooten, J.; Evenhuis, J. K. *Polymer* **1965**, *6*, 343.
(14) Michajlov, L.; Zugenmaier, P.; Cantow, H.-J. *Polymer* **1968**, *9*, 325.
(15) Seeger, M.; Barrall, E. M., II. *J. Polym. Sci., Polym. Chem. Ed.* **1975**, *13*, 1541.
(16) Seeger, M.; Barrall, E. M., II; Shen, M. *J. Polym. Sci., Polym. Chem. Ed.* **1975**, *13*, 1541.
(17) Seeger, M.; Gritter, R. J. *J. Polym. Sci., Polym. Chem. Ed.* **1977**, *15*, 1393.
(18) Ahlstrom, D. H.; Liebman, S. A. *J. Polym. Sci., Polym. Chem. Ed.* **1976**, *14*, 2479.
(19) Mlejnek, O. *J. Chromatogr.* **1980**, *191*, 181.
(20) Private communication (Liebman, S. A.; Ahlstrom, D. H.; Starnes, W. H., Jr.; Schilling, F. C. The Third International Symposium on PVC, Cleveland, Ohio, 1980).
(21) Sugimura, Y.; Tsuge, S. *Macromolecules* **1979**, *12*, 512.
(22) Tsuge, S.; Sugimura, Y.; Nagaya, T. *J. Anal. Appl. Pyrolysis* **1980**, *1*, 221.

Inverse Gas Chromatography Studies of Poly(dimethylsiloxane)–Polycarbonate Copolymers and Blends

T. C. Ward,* D. P. Sheehy, J. S. Riffle, and J. E. McGrath

Chemistry Department and Polymer Materials and Interface Laboratory, Virginia Polytechnic Institute and State University, Blacksburg, Virginia 24061.

Received April 10, 1981

ABSTRACT: The specific retention volumes of a series of volatile probes on stationary phases consisting of homopolymers of poly(dimethylsiloxane) (PDMS) and bisphenol A polycarbonate (PC) as well as block copolymers and blends of these substances were evaluated in terms of the Flory–Huggins approximation. The polymer–solvent, χ_{12}, and normalized polymer–polymer, χ_{23}', noncombinatorial free energies of mixing were determined in each case. χ_{23}' was studied as a function of block length of PC in the copolymer, the chemical structure of the probes, and the copolymer or blend composition. In addition, the morphologies of phase-separated copolymers were analyzed from the specific retention volumes of *n*-decane, a solvent for PDMS and a nonsolvent for PC, at temperatures below the polycarbonate glass transition. The data obtained were compared to morphological information obtained from differential scanning calorimetry, electron microscopy, and small-angle X-ray scattering. Measured χ_{23}' values reflected in all cases the known incompatibility of PDMS and PC in the copolymers and blends. Also, useful information on the copolymers' morphology was obtained by studying the retention behavior of the *n*-decane probe below the PC glass transition. The specific retention volume for the microphase-separated copolymers under these conditions indicated whether the PDMS phase was continuous or not and, in some cases, the actual surface area of the PC domains. Diameters of domains (assuming rod or lamellar geometry) ranging from 180 to 700 Å were calculated from the results.

Introduction

The study of the thermodynamics of interaction between a stationary homopolymer and a volatile probe molecule by gas chromatography[1] (IGC) has been extended to the study of ternary systems containing blends of two nonvolatile components and a volatile probe. Truly miscible mixtures, such as poly(vinyl chloride)–poly(ε-caprolactone)[2] and polystyrene–poly(vinyl methyl ether)[3] have been analyzed in terms of the Flory–Huggins theory to determine the well-known interaction parameters χ_{12}, χ_{13}, $\chi_{1(23)}$, and finally χ_{23}, the noncombinatorial parts of the free energy of mixing, where 1 designates the volatile probe. Hence, χ_{23} is directly related to polymer–polymer compatibility.

Recently, inverse gas chromatography (IGC) has been used to study microphase separation phenomena and domain size in block copolymers containing fundamentally incompatible components.[4,5] Basic thermodynamic quantities of such systems were also estimated. Galin and Rupprecht have successfully analyzed domain sizes in poly(dimethylsiloxane)–polystyrene (PDMS–PS) block copolymers by using volatile probes which were chosen specifically to dissolve in only the siloxane phase.[4] In this type of investigation the gaseous probe was passed over the phase-separated stationary polymer which was maintained at a temperature between the T_g's of each phase. Thus, in this particular work the column temperatures were less than 100 °C. Under such conditions the retention of the probe is restricted to adsorption on the glassy phase and bulk absorption in the liquid-like phase. This behavior, along with the assumption that the accessibility of the probe molecule to each phase is not influenced by the presence of the other, allows one to calculate the surface area of the liquid–glassy interface by measuring the partition coefficent for surface adsorption on the glassy

0024-9297/81/2214-1791$01.25/0